PB87-175824

Interspecies Dosimetry of Reactive Gases

(U.S.) Health Effects Research Lab.
Research Triangle Park, NC

Mar 87

U.S. Department of Commerce
National Technical Information Service
NTIS

PB87-175824

EPA/600/D-87/105
March 1987

INTERSPECIES DOSIMETRY OF REACTIVE GASES

F.J. Miller[1,3], J.H. Overton[1], T.R. Gerrity[1] and R.C. Graham[2]

[1]U.S. Environmental Protection Agency, Health Effects Research Laboratory, Research Triangle Park, NC 27711

[2]Northrop Services Inc.- Environmental Sciences Research Triangle Park, NC 27709

[3]Person to whom correspondence should be addressed.

HEALTH EFFECTS RESEARCH LABORATORY
OFFICE OF RESEARCH AND DEVELOPMENT
U.S. ENVIRONMENTAL PROTECTION AGENCY
RESEARCH TRIANGLE PARK, NC 27711

REPRODUCED BY
U.S. DEPARTMENT OF COMMERCE
NATIONAL TECHNICAL
INFORMATION SERVICE
SPRINGFIELD, VA 22161

TECHNICAL REPORT DATA *(Please read Instructions on the reverse before completing)*		
1. REPORT NO. EPA/600/D-87/105	2.	3. RECIPIENT'S ACCESSION NO. PB87 175824/AS
4. TITLE AND SUBTITLE Interspecies Dosimetry of Reactive GAses		5. REPORT DATE March 1987 6. PERFORMING ORGANIZATION CODE
7. AUTHOR(S) F.J. Miller, J.H. Overton, T.R. Gerrity, R.C. Graham		8. PERFORMING ORGANIZATION REPORT NO.
9. PERFORMING ORGANIZATION NAME AND ADDRESS U.S. EPA, Health Effects Research Laboratory Research Triangle Park, NC 27711 Northrop Services - Environmental Sciences Research Triangle Park, NC 27709		10. PROGRAM ELEMENT NO. 11. CONTRACT/GRANT NO.
12. SPONSORING AGENCY NAME AND ADDRESS Health Effects Research Laboratory - RTP Office of Research and Development U.S. Environmental Protection Agency Research Triangle Park, NC 27711		13. TYPE OF REPORT AND PERIOD COVERED 14. SPONSORING AGENCY CODE EPA/600/11
15. SUPPLEMENTARY NOTES		

16. ABSTRACT

The development of dosimetry models that can provide a description of the uptake and distribution of inhaled compounds throughout the body and the availability of animal toxicological data are integral components for a full evaluation of potential risks associated with human exposure. Interspecies dosimetric comparisons must be approached using a model conceptualization that incorporates the major factors affecting the uptake of the gas, such as respiratory tract morphology, route of breathing, depth and rate of breathing, physicochemical properties of the gas, etc. When studying the lower respiratory tract uptake of highly reactive gases, additional complexities are introduced in treating mass transport since variations in thickness and biological composition of the airway lining can yield a significantly altered dose to the underlying tissue compared to the net mass removed in an airway. Modeling efforts thus far have primarily focused on ozone. A comparison of theoretical predictions of delivered dose of ozone to the lower respiratory tract of man shows good agreement with dose estimates derived from experimental measurements. Applications to ozone toxicological data in animals and man have been examined that incorporate the use of dosimetry models in studying quantitative dose-response relationships.

17. KEY WORDS AND DOCUMENT ANALYSIS		
a. DESCRIPTORS	b. IDENTIFIERS/OPEN ENDED TERMS	c. COSATI Field/Group
18. DISTRIBUTION STATEMENT RELEASE TO PUBLIC	19. SECURITY CLASS (This Report) UNCLASSIFIED	21. NO. OF PAGES 35
	20. SECURITY CLASS (This page) UNCLASSIFIED	22. PRICE

NOTICE

This document has been reviewed in accordance with U.S. Environmental Protection Agency policy and approved for publication. Mention of trade names or commercial products does not constitute endorsement or recommendation for use.

Introduction

The development of dosimetry models that can provide a description of the uptake and distribution of inhaled compounds throughout the body is an integral component of the risk assessment process. The availability of such models allows for more informed judgments of potential risk from human exposure since toxicological data obtained in a variety of animal species using different exposure regimens can be compared to humans on the basis of dose delivered to the target site. This also enables information from studies that are comparable, from a delivered dose perspective, to be assessed collectively, thereby increasing the likelihood that the interpretation of the toxicological results will be correct. Knowledge of the respiratory tract dosimetry of inhaled reactive gases is particularly important since due to their reactivity, they often bind to target sites within the respiratory tract, causing toxicity.

Interspecies dosimetric comparisons of reactive gases must be approached using a model conceptualization that incorporates the major factors affecting the uptake of the gas. Among these factors are respiratory tract morphology, route, rate, and depth of breathing, physicochemical properties of the gas, the physical processes governing gas transport, and the physical and chemical properties of the liquid lining and tissue of the airways and gas exchange units. These various factors interact in a complex manner to determine dose and must be considered in developing mathematical dosimetry models.

Despite the difficulties in developing physiologically-based mathematical dosimetry models, their desirability is without question.

Experimental data on the uptake of reactive gases is limited, in part due to needing to use radiolabeling or isotopic ratio mass spectroscopy techniques to determine delivered dose to specific target sites. Even as improved methods become available for use in experimental studies of the regional dosimetry of reactive gases, there are many exposure scenarios for which it is not practical to obtain experimental data. This does not minimize the need to obtain more experimental measurements of gas uptake. On the contrary, experimental data are critically needed for validation and refinement of theoretical dosimetry models, as well as for determining health effects.

Typically, the proportion of the total toxicological data for inhaled pollutants represented by epidemiological and human clinical studies is small compared to the proportion available from studies using animals. This imbalance stems from the nature and inherent limitations of epidemiological and human clinical studies. Because of confounding variables, it is difficult for epidemiological investigations to quantitatively identify pollutants and the exposure patterns which cause disease. Clinical studies cannot employ chronic exposures and usually require the use of noninvasive techniques, thereby greatly limiting the assessment of potential effects in man. In contrast, animal studies can provide a fuller evaluation of disease, since a wide range of concentrations, exposure regimens, pollutants, and biological endpoints can be employed. However, quantitatively relating effective pollutant exposure concentrations in animals to those for man is difficult. Realizing

that the ultimate use of experimental or theoretical absorption data is to allow concentration-response curves to be converted to dose-response curves for the purposes of intra- and interspecies comparisons of toxicological results, mathematical dosimetry models are needed to facilitate the process. Thusfar, modeling efforts for reactive gases have primarily focused on ozone [1-8], although some modeling of the uptake of formaldehyde [9] and nitrogen dioxide [10] has been done. Hence, ozone (O_3) will be used to illustrate the methodologies needed to develop dosimetry models for reactive gases and to examine various aspects of delivered dose.

Ozone Dosimetry Models

Background

A brief overview of previous O_3 models and analyses will be given to provide the reader with a perspective of the development of research in this area. In 1972, McJilton et al. [1] proposed a model for predicting the uptake of O_3 in the human lung. However, since they did not consider chemical reactions of O_3 with constituents of the lining layer of the airways and gas exchange units, the model was more useful for studying the uptake of nonreactive gases. The model structure and illustrations of modeling results have been presented elsewhere [3, 4]. Miller [2] incorporated an instantaneous reaction scheme (to account for chemical reactions in the liquid lining of the lung) into a mathematical model that described the transport and removal of O_3 in the lower respiratory tract of laboratory animals and man. Using this model, Miller et al. [5] demonstrated a general similarity in the tissue dose-curves for guinea pigs, rabbits, and man, with the first generation of the

pulmonary region predicted to receive the maximum O_3 dose. Mockros et al. [7] developed a mathematical model for the purpose of examining transport, absorption, and chemical reactions of gases in the lower respiratory tract. The model formulation and prediction of lower respiratory tract uptake of O_3 in man and rabbits are similar to the instantaneous reaction regime model developed by Miller [2] and the dose predictions it yields [2, 5].

Improved treatments of effective dispersion, radial mass transport, the use of pseudo-first-order chemical reactions, and the addition of distinct tissue and blood compartments were features of the modeling studies published in 1985 by Miller and colleagues [6]. They showed that, for the human lung, model simulation results were more sensitive to mucous compartment thickness and reaction rate constant than to transport and blood parameters. In addition, for ventilation levels used in many human clinical studies [11], exercise showed a pronounced effect on pulmonary tissue uptake but little effect on tracheobronchial tissue uptake. Recently, modeling studies by Overton et al. [8] focused on the sensitivity of O_3 uptake in laboratory animal lungs to anatomical and ventilatory parameters. Since airway dimensions change during the breathing cycle, an advancement by Overton et al. [8] was to modify the dosimetry model [6] so that anatomical dimensions vary during the cycle. The anatomical models for rats and guinea pigs that were used showed a qualitative similarity in the shape of the dose versus airway number curves but significant differences in predicted percent total and percent pulmonary uptake. Tissue dose in the centriacinar region was found to decrease with increasing distance from the trachea when lobar specific anatomical models were used.

Concepts and Model Formulation

With the above as a brief overview of modeling results available for O_3, this section will describe relevant aspects of respiratory tract morphology and the formulation of the mathematical dosimetry model. The major features of the structure of the lower respiratory tract (LRT) and their relation to model compartments are illustrated in Figure 1. Figure 1a is a diagram of the tracheobronchial (TB) and pulmonary regions of the human lung. For mathematical modeling purposes, the complex branching pattern of the LRT is often summarized by anatomical models as a sequence of sets of cylinders, as symbolized just below the TB region in Figure 1a. The cylinders correspond to airways; each set of cylinders correspond to a generation. Anatomical models exist for man [12, 13] and animals [14-16] that give the number of airways (cylinders) in each generation and the length and diameter of the model airway in each generation. To complete the definition of the air paths in the LRT, the dimensions of pulmonary ducts and sacs, their number in each pulmonary generation, the number of alveoli, their volumes and surface areas must be available or estimated.

In Figure 1b is a micrograph of the interalveolar septum, illustrating the physical structure of the tissue and capillary features of the pulmonary region that should be considered when developing a dosimetry model. At least 95% of the alveolar epithelial tissue is composed of Type I cells which are very thin, allowing efficient gas exchange. The surface of the epithelial layer is covered with a liquid lining, the average thickness of which is less than 5% of the air blood barrier [17]. Beneath

the epithelial layer is the interstitium followed by the endothelial cells that make up the wall of the capillaries. As illustrated in Figure 1b, capillary blood is sandwiched between the air blood barrier that consists mainly of a liquid lining, Type I cells, interstitium, and endothelial cells. Figure 1d is the model formulation of Miller et al [6] for this arrangement in which the epithelium, interstitum, and endothelium have been combined into a single tissue compartment.

A diagram of the structure of the liquid lining and tissue of the TB region considered relevant for modeling O_3 uptake is shown in Figure 1c. The liquid lining is made up of two layers, the epiphase and the hypophase. The former is composed of highly viscous mucus of varying thickness; as is illustrated, the layer may not completely cover the hypophase. The hypophase is a watery-like fluid in which are cilia moving back and forth in such a way as to propel the overlying mucus towards the trachea. The epithelial layer is made up of many cell types, the major types being illustrated in the figure. In the Miller et al. [6] dosimetry model formulation for the TB, the liquid lining layers have been combined into one compartment and the cells into one tissue compartment (see Figure 1e). A blood compartment in the TB region is not needed for O_3 since chemical reactions prevent any significant amount of O_3 from penetrating that deep [6].

In the dosimetry model of Miller et al. [6] and Overton et al. [8], the processes of transport and chemical reactions are described in terms of differential equations. Transport in the lumen of the airways and in the airspaces is described by a time dependent partial differential equation that accounts for axial convection,

axial dispersion, molecular diffusion, the loss of O_3 to the liquid lining, and lung expansion and contraction due to breathing.

$$(1) \qquad \frac{\partial C}{\partial t} + U \frac{\partial C}{\partial x} = D \frac{\partial^2 C}{\partial x^2} - \frac{S}{V} J_W - \frac{\dot{V}}{V} C.$$

In Eq (1), C is the average cross-sectional concentration at position x along a path in the lumen of the airways or airspaces at time t. U is the average air velocity along the x direction; D is the dispersion coefficient; S and V are surface area and volume of the air compartment of the relevant generation; $\dot{V}$ is the time rate change of the volume. J_w is the flux of O_3 to the liquid lining interface and is defined as

$$(2) \qquad J_w = k_g (C - H C_{li}).$$

Henry's law constant, the gas phase mass transfer coefficient, and the liquid lining interfacial concentration of O_3 are respectively, H, k_g, and C_{li}.

The processes considered for the liquid, tissue, and capillary blood compartments are molecular diffusion and chemical reactions. Chemical reactions are assumed to be first order, O_3 reacting only with the unsaturated fatty acids that are assumed to have a constant concentration that depends on the compartment. Because the rates of chemical reactions are much faster than changes in O_3 concentrations due to other processes, the steady state approximation is used [6]. Thus, the equation used to describe the transport and loss of O_3 due to chemical reactions is,

$$(3) \qquad D_j \frac{\partial^2 C_j}{\partial y^2} = k_{lj} C_j.$$

The subscript, j, indicates the liquid lining, tissue or blood compartment; y is the distance perpendicular to the interface between compartments; C_j is the O_3 concentration at y; D_j is the molecular diffusion coefficient; k_{1j} is the first order rate constant. The value of this constant is equal to the product of the second order rate constant of the reaction of O_3 with unsaturated fatty acids and the concentration of the unsaturated fatty acids.

Analytical solutions are obtained from Eq. (3) for each compartment; solutions are matched at the compartment boundaries by using partition coefficients to relate interfacial concentrations and by requiring the flux of O_3 across boundaries to be continuous; the flux is assumed zero midway between the boundaries of the blood compartment. From the solutions, a mass transfer coefficient is obtained for the combined effect of the compartments. Given the compartmental mass transfer coefficient, and Eq.(2), and the boundary and initial conditions, then Eq (1) is solved numerically to obtain the quantity of O_3 absorbed and the dose of absorbed O_3 in each compartment and generation of the LRT. In the model formulation described above, the processes are linear. Hence, the LRT dose will be proportional to the concentration of O_3 entering the trachea.

Intra- and Interspecies Dosimetry of O_3

For discussion of comparative dosimetry, three types of illustrations are presented in this section. (1) An interspecies comparison of tissue dose curves is made, consisting of a plot of the tissue and net dose curves of man, rat, guinea pig, and rabbit versus lung generation. (2) Experimental LRT uptake data is

compared to predicted uptake data. Plots are shown for net O_3 uptake per breath versus tidal volume and versus minute volume. (3) O_3 dose-response curves are constructed using forced expiratory volume in 1 sec (FEV_1) data from a controlled human exposure study and using lavage fluid protein (LFP) data from animal studies. For the former, plots of FEV_1 versus estimated pulmonary tissue dose are presented; for the latter, a graph of LFP versus estimated pulmonary tissue dose for the three animals are shown, allowing a comparison of results for all three animals species.

In order to use the dosimetry model to estimate the dose of O_3 that an exposed animal or man received, information that is needed includes the O_3 concentration, the length of time exposed, as well as the tidal volume (V_T) and breathing frequency (f) during exposure. Usually, all of this information is not reported, and the missing data must be estimated. For example, the ventilatory parameters for laboratory animals are often not measured; however, if the weight of the animals is reported, allometric equations can be used to estimate the absent parameters. Once all of the necessary data have been obtained, either as reported or estimated, then estimated doses can be computed using the mathematical dosimetry model. Using the parameters that characterize the particular animal and the conditions of exposure, the model is used to compute the dose for single or multiple breaths for the length of time necessary. If, during the time of exposure, conditions change (e.g., concentration, ventilatory parameters), then dose for these time periods is estimated using the model. Using the estimated doses and the times of exposure, the total estimated dose is computed. The dosimetry model yields dose per breath in several forms, including

the quantity of O_3 absorbed per unit airway surface area in a given generation, quantity absorbed by region, quantity absorbed by region and compartment (tissue, liquid lining, blood). Given the experimental effects data, a plot of the effects versus the time integrated dose (e.g., TB tissue dose, pulmonary tissue dose, total LRT uptake, etc.) can then be constructed.

Interspecies LRT Dosimetry Patterns

An example of LRT dose curves is illustrated in Figure 2A and 2B in which are plotted net and tissue O_3 dosimetry simulation data versus generation for rat and man, order for guinea pig, and zone for rabbit. (The particular segmentation of airways and ducts into generation, order and zone depends on the anatomical model.) Dose is expressed as micrograms of O_3 per square centimeter of segment (generation, order or zone) surface area per minute, standardized to a tracheal O_3 value of 1 $\mu g/m^3$. Thus, for a tracheal concentration of one part per million, multiply the plotted values by 1960 ($\mu g/m^3$ per ppm).

Because the number of sequential segments are different for all the anatomical models, there is a set of segment indices for each animal along the horizontal axis in Figure 2. Although the predicted doses for each segment are calculated only for each segment of an anatomical model, the data for each species has been joined by lines to help in interpreting the plots. Further, we have matched the tracheas, the last TB segment (terminal bronchioles in the human and rat anatomical models; not defined for the guinea pig and rabbit anatomical models), the last pulmonary segment (defined as sacs in the human, rat and rabbit anatomical models; guinea pig's last order contains sacs and ducts), and the first

airway of respiratory bronchioles in man with the first alveolated airway in the animal lungs. This latter location is where the histopathological data show the first and the most pronounced lesions in O_3 studies using rats [18-22] and monkeys [23-27]. The maximal tissue dose in man, rat, and guinea pig is predicted to occur in this region (Figure 2B). As can be seen from the figures, the shape of the dose curves of O_3 is very comparable in the lungs of these animal species and man. For the same unit tracheal O_3 value, almost a 3-fold increase in the absorption or removal of O_3 is predicted in the first nonciliated portion of the rat lung compared to man. However, the relative doses depend on the ventilatory parameters chosen.

To make more definitive interspecies dosimetric comparisons, upper respiratory tract removal of O_3 in man versus rat must be considered. Preliminary results of O'Neil et al. [28] indicate that upper respiratory tract removal of O_3 in man is about 40-45%. In contrast, Wiester et al. [29] have shown that total respiratory tract removal of O_3 in the rat is only about 40%. Uptake studies are currently being conducted, and unconfirmed preliminary experiments (Drs. Jean Wiester and Gary Hatch, personal communication, indicate that the rat may remove only 10-25% of the inhaled O_3 in the nasopharyngeal region). Further analyses presented in this paper will assume upper respiratory tract removal values of 20% for rats, guinea pigs, and rabbits, and 40% for man.

Experimental LRT Data and Theoretical Predictions

The O_3 removal efficiency of the lower respiratory tract was measured in healthy non-smoking male volunteers [28]. A small

polyethylene tube was inserted through a subject's nostril until the tip of the tube could be visualized orally 0.5 cm below the soft palate. While a subject was seated in an environmental O_3 exposure chamber, samples of air from the posterior pharynx were drawn through the tube and into an O_3 analyzer (Monitor Labs 8410) that had been modified so that it could respond rapidly to changing O_3 concentrations. Samples of air from the posterior pharynx were collected while the subject was exposed to either 0.1, 0.2, or 0.4 ppm. At each concentration a subject breathed at a breathing frequency of either 12 or 24 breaths per min (bpm), and either through his nose only, mouth only, or oronasally. Ventilation (f and V_T) was measured concurrently with pharyngeal O_3 concentration. Data were collected from each subject at all combinations of O_3 concentration, mode of breathing, and breathing frequency utilizing a randomized split-split-plot design. The O_3 removal efficiency, F, of that part of the respiratory tract distal to the posterior pharynx (ALRT; the LRT augmented by the segment of the respiratory tract from the posterior pharynx to the trachea) was calculated by dividing the O_3 concentration in the posterior pharynx during expiration by the O_3 concentration during inspiration and subtracting this from unity.

The mean O_3 removal efficiency of ALRT over all subjects, O_3 concentrations, modes of breathing, and breathing frequencies was 0.910 ± 0.005 (SEM). The mass dose of O_3 to the ALRT was computed for each combination of subject, O_3 concentration, mode of breathing, and breathing frequency,and compared with the dosimetry model predictions for ALRT total dose. Figure 3 shows the dose of O_3 per breath defined as the product of F, tidal volume (reduced by the

upper respiratory tract volume proximal to the posterior pharynx), and mass concentration equivalent to one ppm plotted against V_T. Figure 4 shows the dose of O_3 per breath per ppm plotted against minute volume ($\dot{V}_E$).

The predicted values are also shown in Figures 3 and 4, indicating good agreement between the dosimetry model predictions and the values based on the measurements. To obtain the predicted values, the Weibel (1963) anatomical model was used but adjusted to a function residual capacity (FRC) of 3.32 liters. According to Morris et al. [30], this is the value that corresponds to the subjects' average age and height of 29 years and 177 cm, respectively. The tidal volume and breathing frequencies used for the simulations were chosen to represent the range of experimental values. All other parameters have the values as given in Miller et al. [6]. The agreement was obtained without adjusting the values of any parameters (such as chemical rate constants, compartment thicknesses, partition coefficients, etc.) except of course, V_T, f and FRC.

When plotted against V_T, the doses per breath fall within a straight band regardless of f; however, when plotted against $\dot{V}_E$, the data split according to whether f was 12 or 24 bpm. The slope of the line at 12 bpm is approximately half that at 24 bpm. These results indicate that V_T is a more important determinant of net dose per breath than is f. In addition, since the dosimetry model predictions of net dose agree well with experimental measurements of total ALRT uptake, it is reasonable to speculate that the LRT dose pattern for man given in Figure 2 may be reflective of that occurring *in vivo*.

Decrements in FEV_1 Versus Pulmonary Tissue Dose in Man

Human clinical studies routinely employ exercise as a part of the experimental regimen in O_3 exposure studies [11]. Probably FEV_1 is the pulmonary function parameter studied most often since this variable reflects a summation of changes in both volume and resistance. However, for O_3 exposures to 0.3 ppm or less, decrements in FEV_1 mainly reflect forced vital capacity changes of similar magnitude, with little to no contribution from resistive changes [11].

A detailed consideration of the numerous clinical studies in which FEV_1 changes have been studied with O_3 levels ranging from 0.11 to 0.75 ppm for $\dot{V}_E$ from 20 to 70 L/min is beyond the scope of this paper (EPA [11] cites 25 such studies involving a total of more than 300 subjects). Rather, this section focuses on one such concentration-response study [31] to illustrate an approach to intraspecies dose-response comparisons. McDonnell and coworkers [31] divided 135 healthy subjects into six groups, each group exposed to a different concentration of O_3 [(ppm, number of subjects): (0, 20), (0.12, 22), (0.18, 20), (0.24, 21), (0.3, 21), (0.4, 29)]. During the first 120 min of the 2.5 hour exposure regimen, alternating 15 min periods of rest and exercise ($\dot{V}_E$ ranging from 64 to 68 L/min) were employed. While still being exposed, forced expiratory spirometry was measured 5 min after the final exercise.

The average age and average height of all subjects were used to obtain a common FRC estimated from [30] to be used for simulating the dose of each exposure group. This was reasonable since the averages were not significantly different from one group to the next. Tidal volumes and breathing frequencies were dependent on the particular

15 min period and exposure groups. Values of these parameters were reported for two exercise periods, as well as were minute volume averaged over the four exercise periods for each group. Using this data, estimated one hour average V_T and f were made for the total time of exercise for each group (estimated average V_T and f ranged from 1820 ml and 35.5 bpm to 2251 ml and 30.2 bpm; $\dot{V}_E$ ranged from 65 to 68 liters per minute). No measurements of ventilatory parameters for the rest periods were reported. For the first rest period, we assumed V_T = 800 ml and f = 15 bpm; for the rest periods after the exercise periods, including the 5 min rest period prior to measurement, we chose V_T = 800 ml and f = 20 bpm.

In Figure 5 are plotted the changes in FEV_1 observed by McDonnell et al [31] against the pulmonary tissue doses predicted by the mathematical dosimetry model after adjusting for upper respiratory tract removal [28]. The dose-response curve is sigmoid in shape and similar to the concentration-response curve of [31]. Differences in the shape of the two curves are due primarily to the number of additional factors, in addition to concentration, for which the dose is dependent and were accounted for in the dosimetry model estimates: upper respiratory tract removal efficiency, V_T and f changes over the exposure period, estimating the amount of O_3 delivered to the portion of the lung to which the FEV_1 changes relate, etc.

Interspecies Effects of O_3 on Lavage Fluid Protein (LFP)

Concentration response studies were conducted by Hatch et al [32] in which groups of rabbits, guinea pigs, rats, hamsters, and mice were exposed for 4 hours to either 0, 0.2, 0.5, 1.0, or 2.0 ppm of O_3. LFP accumulation 18-20 hr after cessation of

exposure was used as an indicator of O_3-induced pulmonary edema. Although the air-exposed animals for all species had similar basal levels of LFP, guinea pigs showed significant effects at 0.2 ppm O_3, mice, hamsters, and rats at 1.0 ppm O_3, and rabbits at 2.0 ppm O_3. There were also species differences in the percent of lavage fluid that could be recovered. The various concentration-response results did not appear to Hatch et al. [32] to be related to species differences in body weight.

The values of the ventilatory parameters and the FRCs were not reported for the animals investigated; however, weight ranges were reported, and we chose the mean of the range as an animal's weight to be used with allometric equations to estimate ventilatory parameters and FRCs. FRC was defined as one-half of the TLC value of each animal, as predicted by the formulae of Takezawa et al. [33]. The equations of Gunther [34] were used to estimate V_T and f.

The LFP concentration-response data reported by Hatch et al. [32] for the guinea pig, rat, and rabbit are depicted as dose-response data in Figure 6. Anatomical models were not available for the hamster and mouse, so dose-response curves were not constructed for these two species. The mathematical dosimetry model estimates of the amount of O_3 delivered to pulmonary tissue over the 4 hr exposure period have been divided by body weight to facilitate interspecies comparisons of possible differences in sensitivity to O_3 exposure. The partial horizontal line at LFP ~470 µg/ml divides the data so that those values below the line are not (statistically) significantly ($p>0.05$) different than the control values (zero dose). The LFP values above the line, including the second guinea pig, but not the fourth rabbit, data point are all significantly different

($p<0.05$) than the control values of LFP. The rats and rabbits respond similarly with the first significantly elevated level of protein corresponding to a pulmonary tissue dose of about 80 ng O_3/g body weight. On the other hand, the first significantly elevated level of protein for the guinea pig occurs at ~12-13 ng O_3/g body weight. These results suggest, that for equivalent pulmonary tissue ozone doses, the guinea pig is more sensitive initially to O_3 than the rat and rabbit. Because of the predicted differences in species sensitivity, speculation as to the effect of equivalent doses in man is not feasible or at best ambiguous. For example, note that the maximal dose to the pulmonary region in the human studies associated with FEV_1 changes in Figure 5 is about 22 ng O_3/g body weight. If man is as sensitive as the guinea pig then we would conclude that there was probably edema formation in the human study. However, if man is more like the rat and rabbit we would predict no edema formation in any of the exposed human subjects. A third possibility, of course, is that man's sensitivity to O_3 is not similar to any of the three laboratory animals.

Summary

We have demonstrated the feasibility of using physiologically-based dosimetry models to enable interspecies comparisons of responses following exposure to reactive gases. Although the specifics of the process and examples of lower respiratory tract dose patterns were presented for the reactive gas, O_3, the intent was to illustrate the type of biological, physical, and chemical information that must be synthesized for the development of dosimetry models that facilitate interspecies comparisons of dose delivered to comparable target

sites. The critical information areas include respiratory tract morphology, route, rate, and depth of breathing, physicochemical properties of the gas, the physical processes governing gas transport, and the physical and chemical properties of the liquid lining and tissue of the airways and gas exchange units. Application of an O_3 dosimetry model to obtain intra- and interspecies dose-response curves highlights the potential impact of dosimetry models for collective assessments of toxicological data, thereby improving the overall risk assessment process, especially its quantitative aspects. Since the full array of potential effects from exposure to inhaled compounds can only be accomplished by integrating information from epidemiological, human clinical, and animal toxicological studies, improvements in our ability to make more quantitative comparisons among species are inextricably linked to an improved understanding of interspecies dosimetry.

Acknowledgement

The authors would like to express their appreciation to Mr. Andrew Barnett for his excellent technical assistance and to Ms. Carolyn Wheeler for her typing of the manuscript.

References

1. McJilton C, Thielke J, Frank R (1972) Ozone uptake model for the respiratory system. In: Abstracts of Technical Papers, American Industrial Hygiene Conference, 14-19 May 1972, paper no 45.

2. Miller FJ (1977) A mathematical model of transport and removal of ozone in mammalian lung. Thesis, North Carolina State University, Raleigh

3. National Research Council (1977) Committee on medical and biological effects of environmental pollutants, subcommittee on ozone and other photochemical oxidants. Toxicology, ozone and other photochemical oxidants, National Academy of Sciences, Washington, DC, p 323-387

4. Morgan MS, Frank R (1977) Uptake of pollutant gases by the respiratory system. In: Brain JD, Proctor DF (eds) Respiratory defense mechanisms Part I. Marcel Dekker, Inc., NY, p 157-189

5. Miller FJ, Menzel DB, Coffin DL (1978) Similarity between man and laboratory animals in regional pulmonary deposition of ozone. Environ Res 17:84-101

6. Miller FJ, Overton, JH, Jr, Jaskot RH, Menzel DB (1985) A model of the regional uptake of gaseous pollutants in the lung. I. The sensitivity of the uptake of ozone in the human lung to lower respiratory tract secretions and exercise. Toxicol Appl Pharmacol 79:11-27

7. Mockros LF, Grotberg JB and Sheth BV (1985) Absorption of noxious gases in pulmonary airways. Abstract from 38th ACEMB Meeting, 30 September to 2 October, Chicago

8. Overton JH, Graham RC, Miller FJ (1987a) A model of the regional uptake of gaseous pollutants in the lung. II. The sensitivity of ozone uptake in laboratory animal lungs to anatomical and ventilatory parameters. Toxicol Appl Pharmacol (in press)

9. Chang JCF, Gross EA, Swenberg JA, Barrow CS (1983) Nasal cavity deposition, histopathology, and cell proliferation after single or repeated formaldehyde exposure in B6C3F1 mice and F-344 rats. Toxicol Appl Pharmacol 68:161-176

10. Miller FJ, Overton JH, Meyers ET, Graham JA (1982) Pulmonary dosimetry of nitrogen dioxide in animals and man. In: Schneider T and Grant L (eds) Air Pollution by Nitrogen Dioxide. Proceedings of US-Dutch International Symposium on NO_x, Maastricht, Netherlands. Elsevier Press, p 377-386

11. U.S. Environmental Protection Agency (1986) Air quality criteria for ozone and other photochemical oxidants. Vol V EPA/600/8-84/020eF August 1986

12. Weibel ER (1963) Morphometry of the human lung. Academic Press, Inc., New York

13. Yeh HC, Schum GM (1980) Models of human lung airways and their application to inhaled particle deposition. Bull Math Biol 42:461-480

14. Kliment V (1973) Similarity and dimensional analysis, evaluation of aerosol deposition in the lungs of laboratory animals and man. Folia Morphol 21:59-64

15. Yeh HC, Schum GM, Duggan MT (1979) Anatomic models of the tracheobronchial and pulmonary region of the rat. Anat Rec 195:483-492

16. Schreider JP, Hutchens JO (1980) Morphology of the guinea pig respiratory tract. The Anatomical Record 196:313-321

17. Weibel ER (1973) Morphological basis of alveolar-capillary gas exchange. Physiol Rev 53(2):419-495

18. Stephens RJ, Sloan MF, Evans MJ, Freeman G (1973) Early response of lung to low levels of ozone. Amer J Pathol 74:31-58

19. Stephens RJ, Sloan MF, Evans MJ, Freeman G (1974) Alveolar type 1 cell response to exposure to 0.5 ppm O_3 for short periods. Exp Mol Pathol 20:11-23

20. Plopper CG, Chow CK, Dungworth DL, Tyler WS (1979) Pulmonary alterations in rats exposed to 0.2 and 0.1 ppm ozone: a correlated morphological and biochemical study. Arch Environ Health 34:390-395

21. Boorman GA, Schwartz LW, Dungworth DL (1980) Pulmonary effects of prolonged ozone insult in rats. Lab Invest 43(2):108-115

22. Barry BE, Miller FJ, Crapo JD (1985) Effects of inhalation of 0.12 and 0.25 ppm ozone on the proximal alveolar region of juvenile and adult rats. Lab Invest 53:692-704

23. Dungworth DL, Castleman WL, Chow CK, Mellick PW, Mustafa MG, Tarkington B, Tyler WS (1975b) Effect of ambient levels of ozone on monkeys. Fed Proc Fed Am Soc Exp Biol 34:1670-1674

24. Castleman WL, Tyler WS, Dungworth DL (1977) Lesions in respiratory bronchioles and conducting airways of monkeys exposed to ambient levels of ozone. Exp Mol Pathol 26:384-400

25. Eustis SL, Schwartz LW, Kosch PC, Dungworth DL (1981) Chronic bronchiolitis in nonhuman primates after prolonged ozone exposure. Am J Pathol 105:121-137

26. Mellick PW, Mustafa MG, Tyler WS, Dungworth DL (1975) Morphologic and biochemical changes in primate lung due to low-level ozone exposure. In: Proceedings of 23rd international tuberculosis conference, September, Mexico. Bull Int Union Tubercul 51:565-567

27. Mellick PW, Dungworth DL, Schwartz LW, Tyler WS (1977) Short term morphologic effects of high ambient levels of ozone on lungs of rhesus monkeys. Lab Invest 36:82-90

28. O'Neil JJ, Gerrity TA, Weaver RA, Berntsen JH, Overton JH, Miller FJ (1987) Ozone removal in the nasopharynx and lungs of normal man during tidal breathing. Abstract from International Symposium on Inhalation Toxicology, 23-27 March, Hannover, W. Germany

29. Wiester MJ, Williams TB, King ME, Ménache MG, Miller, FJ (1987) Ozone uptake in awake Sprague Dawley rats. Toxicol Appl Pharmacol (accepted for publication)

30. Morris AH, Kanner RE, Crapo RO, Gardner RM (1984) Clinical Pulmonary Function Testing. 2nd Edition. International Thoracic Society, Salt Lake City, Utah

31. McDonnell WF, Horstman DH, Hazucha MJ, Seal E, Jr, Haak ED, Salaam S, House DE (1983) Pulmonary effects of ozone exposure during exercise: dose-response characteristics. J Appl Physiol: Respir Environ Exercise Physiol 54:1345-1352

32. Hatch GE, Slade R, Stead AG, Graham JA (1986) Species comparison of acute inhalation toxicity of ozone and phosgene. J Toxicol Environ Health 19:43-53

33. Takezawa J, Miller FJ, O'Neil JJ (1980) Single-breath diffusing capacity and lung volumes in small laboratory animals. J Appl Physiol: Respirat Environ Exercise Physiol 48(6):1052-1059

34. Gunther B (1975) Dimensional analysis and theory of biological similarity. Physiol Reviews 55:659-699

35. Miller FJ, Overton JH, Smolko ED, Graham RC, Menzel DB (1987) Hazard assessment using an integrated physiologically-based dosimetry modeling approach: ozone. National Academy of Sciences (in press).

Figure Legends

1. The relationships between morphologies and their model representations. Panel a is a schematic of the branching airways of the TB and pulmonary region of man. The generations are labeled from the right, beginning with the trachea. BR, BL and TBL indicate bronchi, bronchioles and terminal bronchioles, respectively; the respiratory bronchioles, alveolar ducts, and alveolar sacs are indicated by RBL, AD and AS, respectively. Below the TB portion of the lung schematic are three cylindrical figures that indicate the model representation of the airways. Panel c shows a diagram of the structure of the liquid lining and tissue of the TB region. The different cells represented are basal (BC), ciliated (CC), brush (BrC), goblet (GC), and nonciliated serous (NCC). Panel e illustrates the model representation of TB liquid lining and tissue compartments. On the left side of the figure, Panel b, is an electron micrograph of the interalveolar septa. The air spaces (A), capillaries (C), type I cells and their nuclei (EP1 and NEP1), endothelial cells and their nuclei (EN and NEN), and interstitial space (IN) are indicated. Panel d illustrates the model representation of the liquid lining, tissue and capillaries of the pulmonary region. Figure reprinted from Miller et al [35].

2. Net dose (2A) and tissue dose (2B) versus sequential segments along anatomical model airway paths for man, rat, guinea pig and rabbit. In general each segment represents a group of airways or ducts with common features as defined by the designers of the anatomical model (man: generation [12]; rat: generation [15]; guinea pig: order [16]; rabbit: zone [14]) For a given species the plotted "dots"

represent a predicted dose that corresponds to a given segment. The "dots" have been joined by lines for ease of interpreting the plots; these lines do not represent predicted values except where they intercept the "dots".

3. Dose versus tidal volume. Plotted are the experimental data and the predicted values for the absorption of O_3 in human subjects in that part of the respiratory tract distal to the posterior pharynx. For the predicted values, V_T and f were chosen to encompass the range of experimental ventilatory parameters.

4. Dose versus minute ventilation. Plotted are the experimental data and the predicted values for the absorption of O_3 in human subjects in that part of the respiratory tract distal to the posterior pharynx. For the predicted values, V_T and f were chosen to encompass the range of experimental ventilatory parameters.

5. Changes in FEV_1 versus pulmonary tissue dose. Plotted are decrements in FEV_1 (liters) for human subjects against predicted pulmonary tissue dose normalized to body weight. In order, from left to right, the dose values correspond to 0, 0.12, 0.18, 0.24, 0.30 and 0.40 ppm O_3 exposure concentration. The continuous curve was "eye fit".

6. LFP versus pulmonary tissue dose. Plotted for rat, guinea pig, and rabbit is lavage fluid protein (LFP, µg/ml) against predicted pulmonary tissue dose normalized to animal body weight. For each species, in order from left to right, the dose values correspond to 0.0, 0.2, 0.5, 1.0 and 2.0 ppm O_3 exposure concentration.

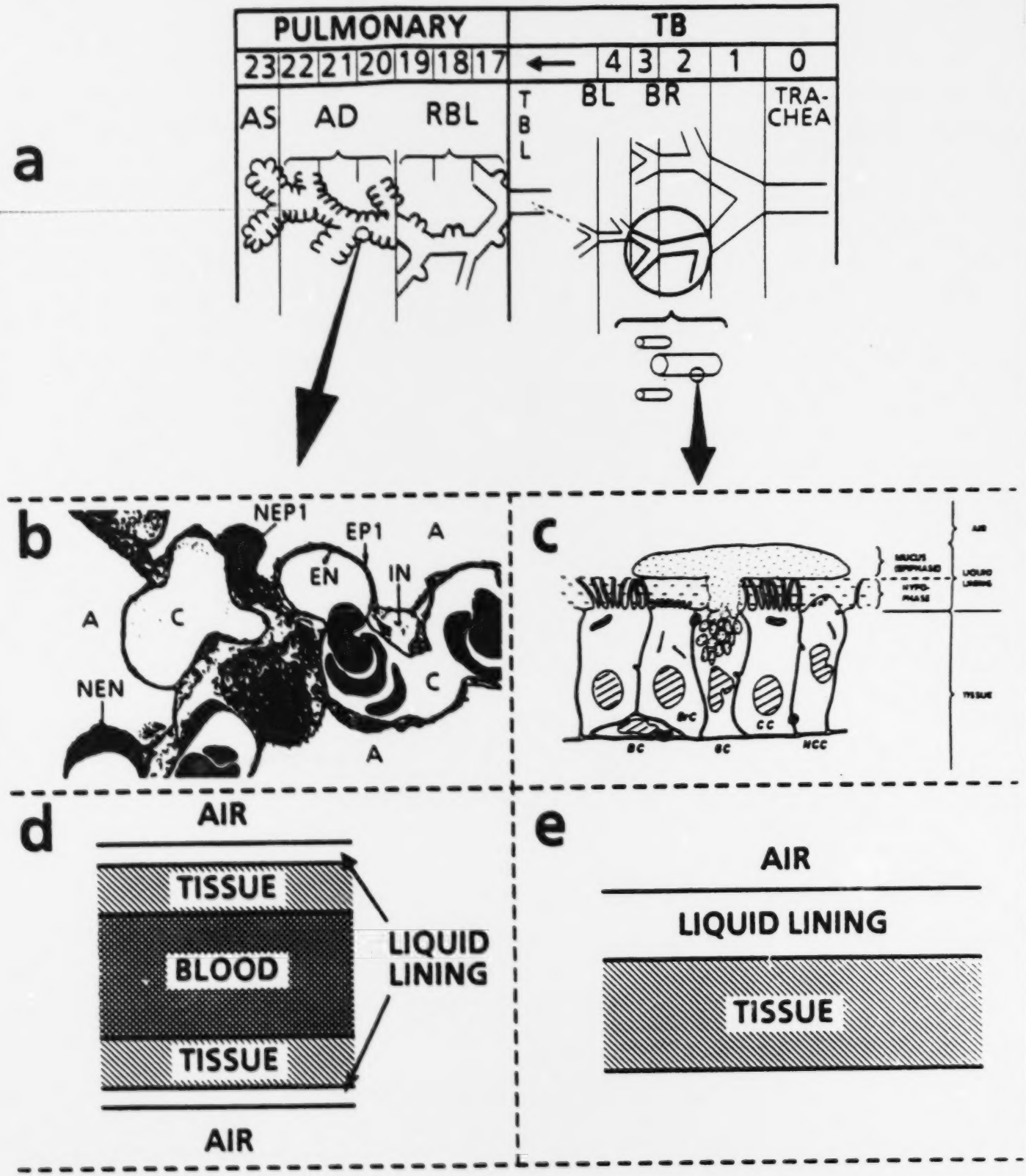
a
PULMONARY
TB
23 22 21 20 19 18 17
4 3 2 1 0
AS
AD
RBL
TBL
BL
BR
TRA-
CHEA
b
NEP1
EP1
A
EN
IN
A
C
NEN
C
A
c
d
AIR
TISSUE
BLOOD
TISSUE
LIQUID
LINING
AIR
e
AIR
LIQUID LINING
TISSUE

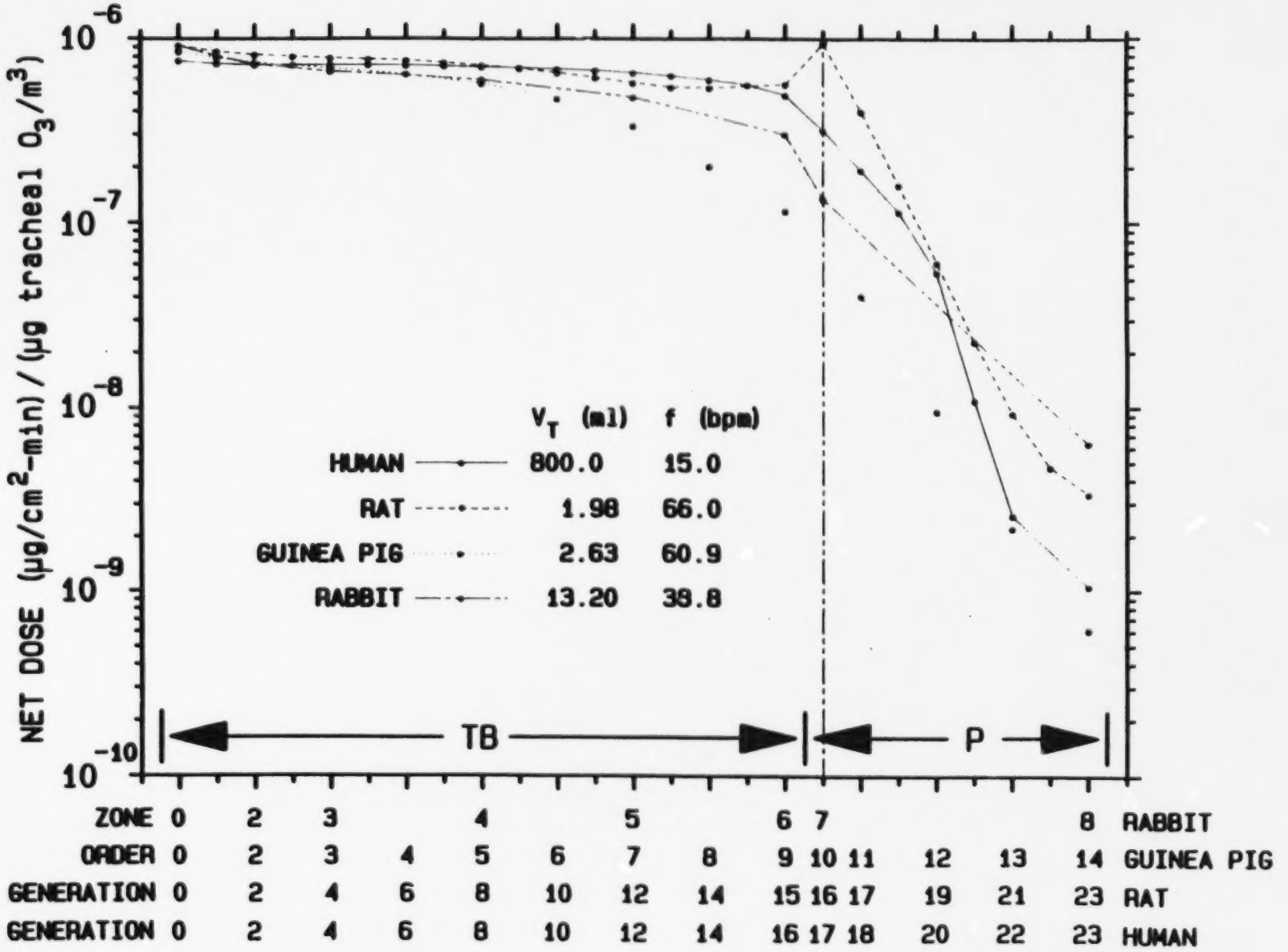
NET DOSE (μg/cm²-min) / (μg tracheal O₃/m³)
10⁻⁶
10⁻⁷
10⁻⁸
10⁻⁹
10⁻¹⁰
V_T (ml) f (bpm)
HUMAN 800.0 15.0
RAT 1.98 66.0
GUINEA PIG 2.63 60.9
RABBIT 13.20 38.8
TB
P
ZONE 0 2 3 4 5 6 7 8 RABBIT
ORDER 0 2 3 4 5 6 7 8 9 10 11 12 13 14 GUINEA PIG
GENERATION 0 2 4 6 8 10 12 14 15 16 17 19 21 23 RAT
GENERATION 0 2 4 6 8 10 12 14 16 17 18 20 22 23 HUMAN

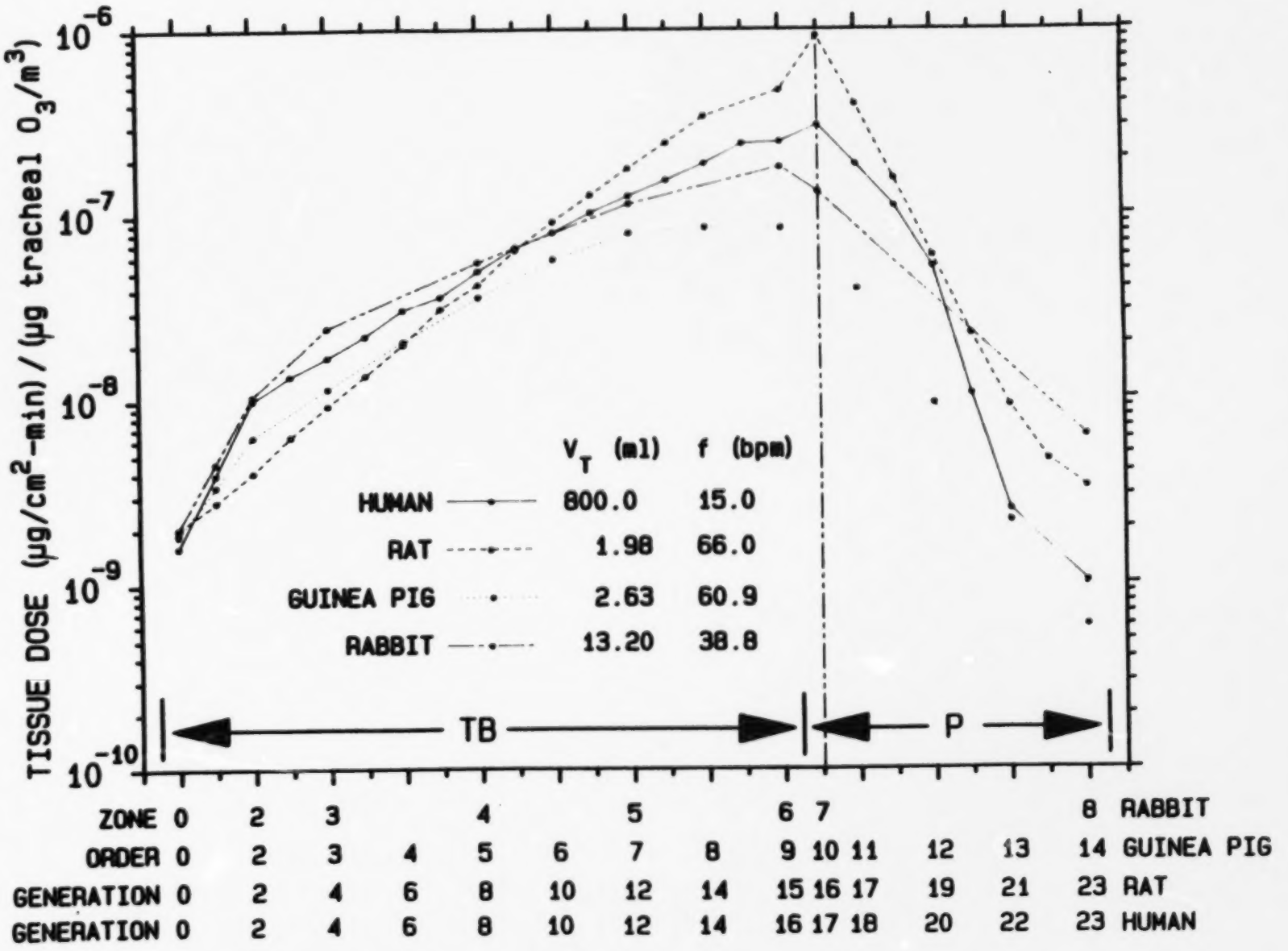
TISSUE DOSE (μg/cm²-min) / (μg tracheal O₃/m³)
10⁻⁶
10⁻⁷
10⁻⁸
10⁻⁹
10⁻¹⁰
V_T (ml) f (bpm)
HUMAN 800.0 15.0
RAT 1.98 66.0
GUINEA PIG 2.63 60.9
RABBIT 13.20 38.8
TB
P
ZONE 0 2 3 4 5 6 7 8 RABBIT
ORDER 0 2 3 4 5 6 7 8 9 10 11 12 13 14 GUINEA PIG
GENERATION 0 2 4 6 8 10 12 14 15 16 17 19 21 23 RAT
GENERATION 0 2 4 6 8 10 12 14 16 17 18 20 22 23 HUMAN

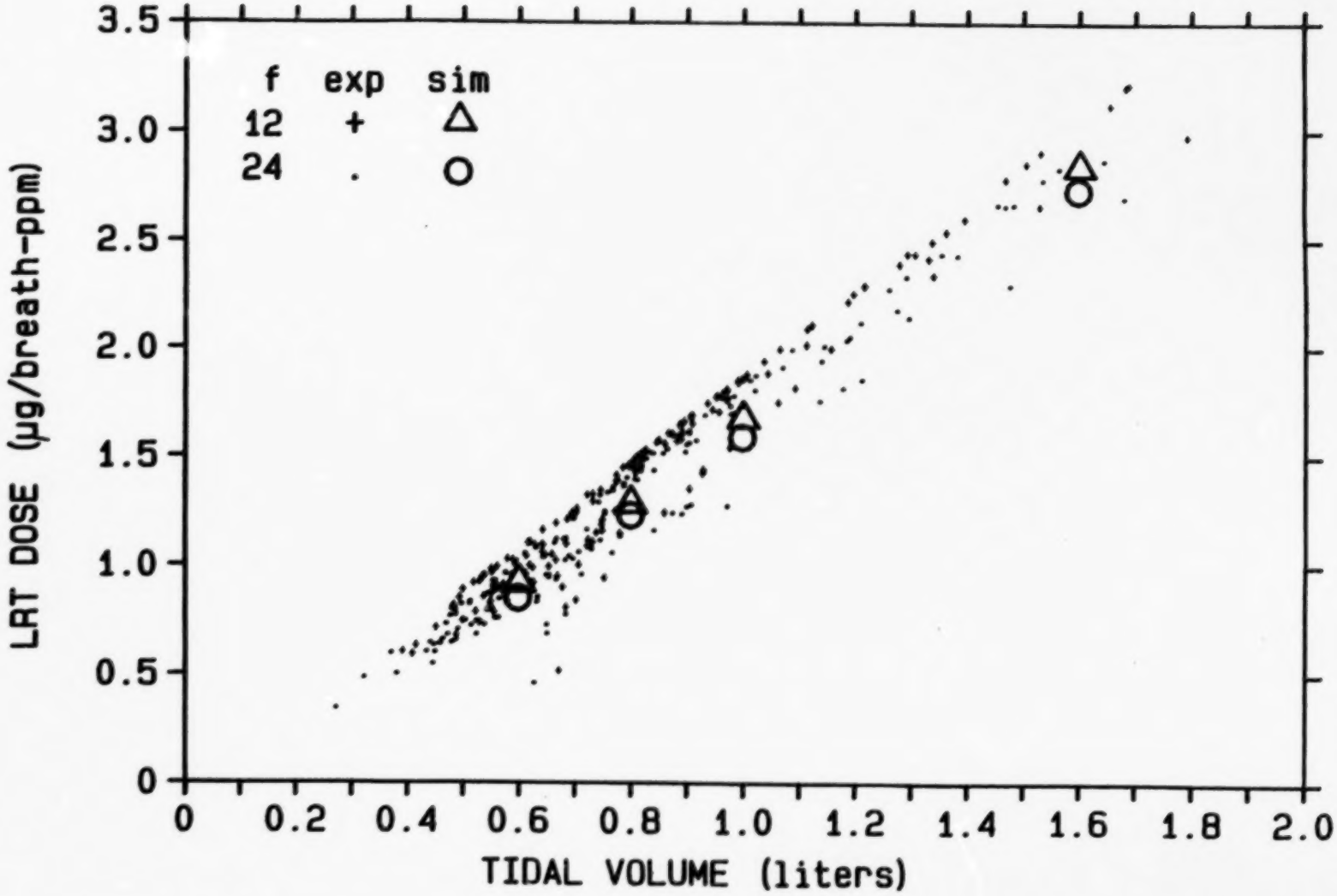
f exp sim
12 + △
24 . ○
LAT DOSE (µg/breath-ppm)
TIDAL VOLUME (liters)
0
0.5
1.0
1.5
2.0
2.5
3.0
3.5
0.2
0.4
0.6
0.8
1.0
1.2
1.4
1.6
1.8
2.0

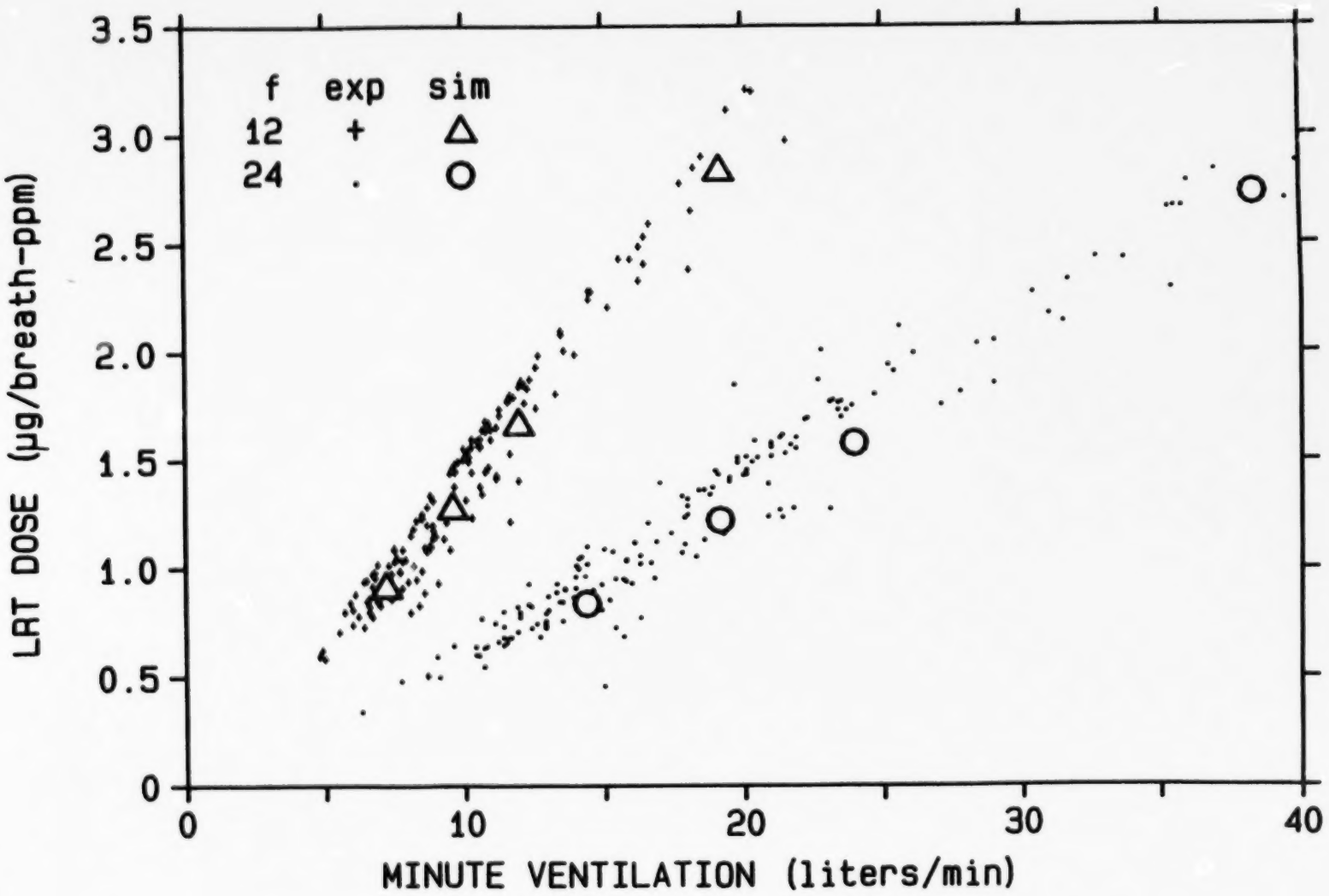
f exp sim
12 + Δ
24 . O
LAT DOSE (µg/breath-ppm)
MINUTE VENTILATION (liters/min)
0
0.5
1.0
1.5
2.0
2.5
3.0
3.5
0
10
20
30
40

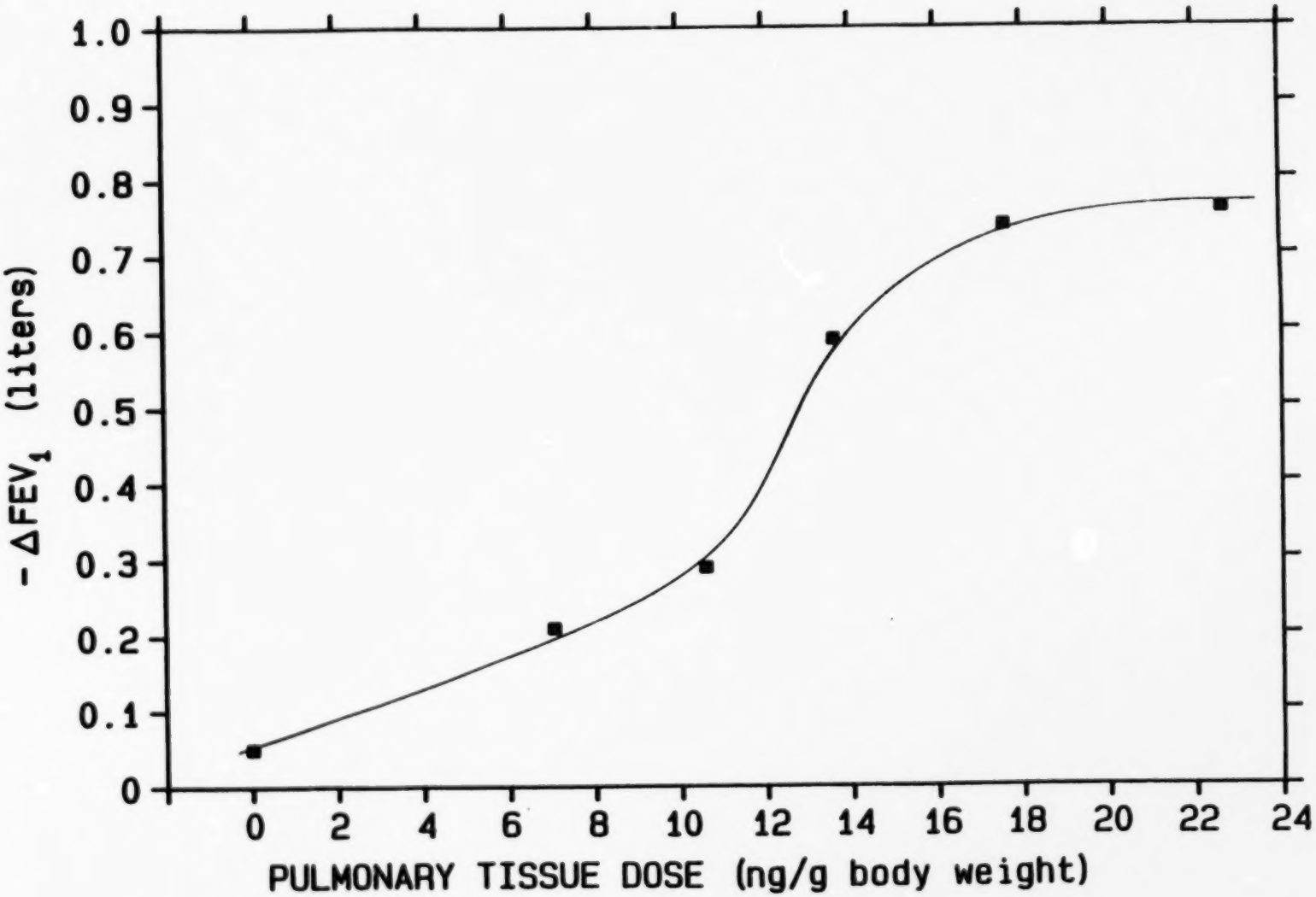
1.0
0.9
0.8
0.7
0.6
0.5
0.4
0.3
0.2
0.1
0
- ΔFEV1 (liters)
0
2
4
6
8
10
12
14
16
18
20
22
24
PULMONARY TISSUE DOSE (ng/g body weight)

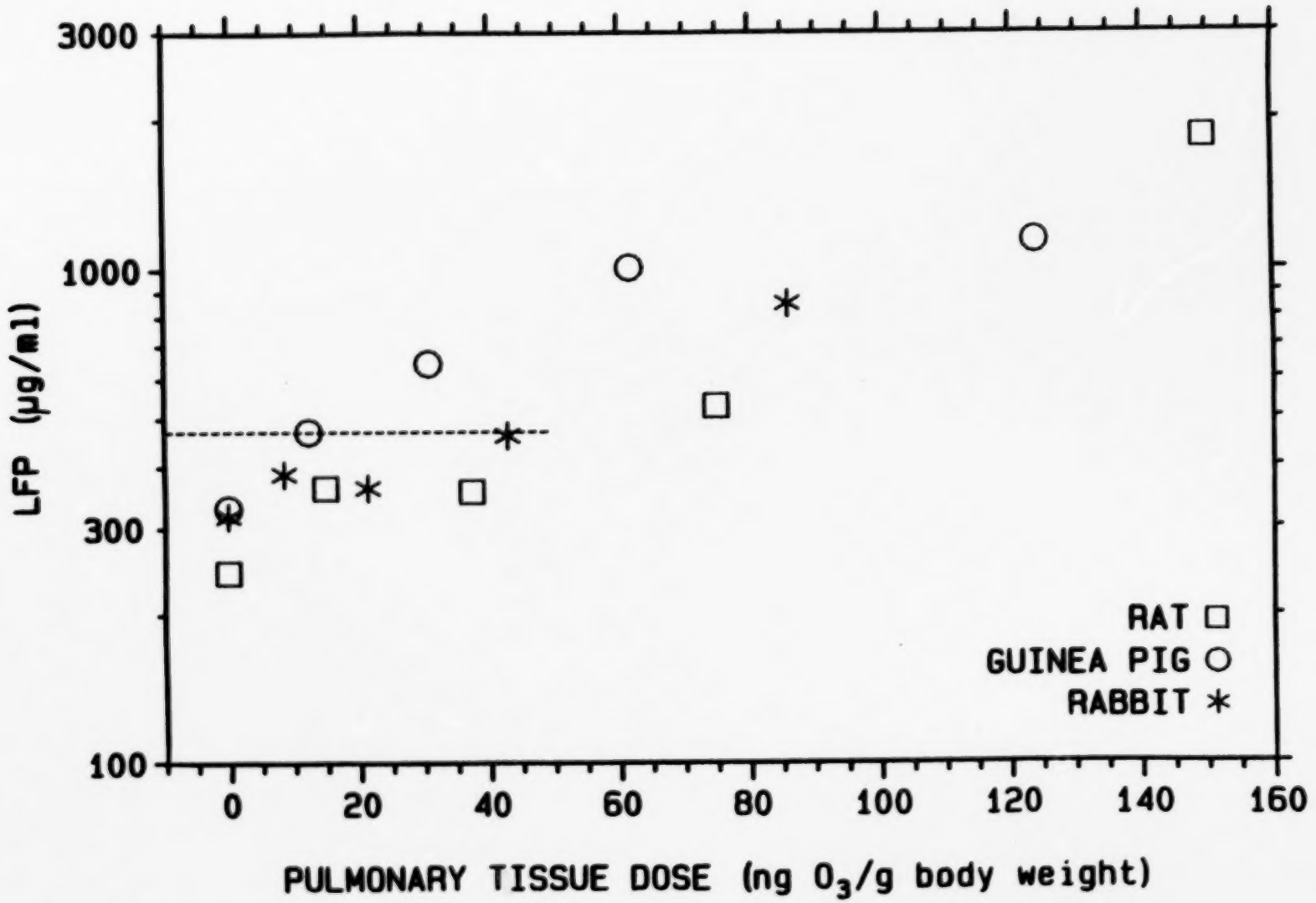
3000
1000
300
100
LFP (µg/ml)
0
20
40
60
80
100
120
140
160
PULMONARY TISSUE DOSE (ng O_3/g body weight)
RAT □
GUINEA PIG ○
RABBIT *